Electric potential of the electron sound wave: Sharp disappearance in the superconducting state

Yu. A. Avramenko, E. V. Bezuglyi, N. G. Burma, and V. D. Fil

B. Verkin Institute for Low Temperature Physics and Engineering, National Academy of Sciences of Ukraine, 47 Lenin Ave.,
Kharkov UA-61103, Ukraine

We study the ac electric potential induced by the electron sound wave (a perturbation of the electron distribution function propagating with the Fermi velocity) in single crystals of high-purity gallium. The potential and the elastic components of the electron sound demonstrate qualitatively different dependencies on the electron relaxation rate: while the phase of the potential increases with temperature, the phase of elastic displacement decreases. This effect is explained within the multiband model, in which the potential is attributed to the ballistic quasiwave, while the elastic component is associated with the zero-sound wave. We observed a mysterious property of the superconducting state: all manifestations of the potential accompanying the lattice deformations, including usual sound wave, disappear below T_c in almost jumplike manner.

I. INTRODUCTION

Longitudinal perturbations of the electronic and elastic subsystems of metals are accompanied by fluctuations of the electron density and occurrence of alternating electric fields, which provide electrical neutrality of the system. The ac electric potential of a longitudinal sound wave has been first measured in Ref. [1]; it should be distinguished from the nonlinear dc potential arising due to the dragging effect.[2–4] In metals, besides the acoustic mode, there exists several types of electron sound, i.e., longitudinal oscillations of the electron distribution function, propagating with nearly Fermi velocity and coupled to elastic deformations and electric fields: acoustic plasmons,[5] ballistic quasiwaves,[6] and zero sound.[7–11] The study of these fast modes gives important information about the mechanisms of electron relaxation, spectrum of the Fermi velocities and Fermi-liquid correlation function in metals.[10–15]

In the experiments mentioned above, excitation of the electron sound has been performed by a high-frequency elastic deformation of the sample surface. As a result, both the acoustic and the electron sound waves were simultaneously excited in the bulk of the sample. These waves can be easily separated in the time-of-flight experiment; the signal φ_S, which comes with the sound delay, will be referred to below as "sound potential," and the signal φ_{ES} propagating with the Fermi velocity will be called "electron sound potential." It should be noted, however, that the potential as well as the elastic displacement are measured at the metal boundary, where partial conversion between different types of the oscillations always occurs. Therefore the recorded signal is generally the result of interference between different processes, and its magnitude may differ from its bulk value in the propagating wave. Indeed, an analysis of the electric signals of the first type, assuming specular reflection of electrons from the sample surface, showed[1] that the potential φ_S is formed by two contributions: φ_q, which has the sound spatial period, and φ_{qw}, generated by the fast quasiwave excited at the receiving interface. Diffuseness of the sample boundary numerically modifies the effect, but the main features remain qualitatively unchanged.[16]

Elastic deformations coupled to the electron sound have been studied in Refs. [10–15] and [17]. In the present paper, we

pay our main attention to the electron sound potential φ_{ES}. This study is of interest due to the following reasons. First, it provides additional arguments in favor of earlier assumptions[10,11] of Fermi-liquid nature of the electron sound, enabling us to separate the zero-sound mode from the quasiwave. Furthermore, the behavior of φ_{ES} in the superconducting state is a topic of particular interest. The earlier study of φ_S has revealed a quite unexpected effect:[1] the sound potential disappeared almost abruptly below T_c. In the present study, we found a similar effect for the potential φ_{ES} of the electron sound, it also abruptly disappears below T_c, though its elastic component changes more smoothly in the superconducting state. Such a behavior of φ_S and φ_{ES} has no explanation within the existing knowledge about the penetration of the longitudinal electric field in superconductors.[18] It can be thought that the mysterious behavior of the electric field generated by an inhomogeneous elastic deformation in a superconductor is a common property of the superconducting phase irrespective of investigated materials.

The paper is organized as follows. In Sec. II, we present the measured temperature dependencies of the modulus and the phase of the signals. In Sec. III, we examine various theoretical models that describe formation of φ_{ES} for both diffusive and specular interfaces. We conclude that the theory of elasticity of metals[19] applied to multiband metals satisfactorily describes the behavior of φ_{ES} and φ_S in the normal state. The results for the superconducting state are presented in Sec. IV.

II. EXPERIMENTAL SETUP AND RESULTS IN THE NORMAL STATE

The experimental setup was the same as described in Refs. [1] and [14]. One of the faces of a high-purity gallium single crystal (impurity mean free path $\sim$5 mm) was excited through the delay line by a longitudinal elastic wave with the frequency of 55 MHz and the diameter of the sound beam $\sim$4 mm. The elastic component of the signal at the opposite face of the sample was registered by a piezoelectric transducer, and the electric potential was measured by an electrode attached to the sample within the region of the "sound spot." The

electrode has been made from the sound-absorbing material (brass) to prevent appearance of its own potential. In contrast to Ref. 1, where we used a point contact, the electrode diameter was 2.5 mm, which provides more controlled mechanical boundary conditions. The electrode can be glued to the sample surface by the acoustic grease or slightly appressed to the sample by a spring. Obviously, the first case is more similar to a matched boundary, while the second case to a free one. The experiment was performed in the time-of-flight regime; the duration of the excitation signal has been chosen smaller than the sound delay in the sample, which excludes the possibility of the acoustic resonance. The electron sound resonance was suppressed due to diffusive scattering of electrons at the sample boundaries.

In all cases, we detected two types of signals: fast modes propagating with the Fermi velocity (electron sound) and slow ones having the sound velocity. The elastic component u_{ES} of the electron sound was about of 80 dB lower than its value u_S in the acoustic signal, while the magnitudes of the potentials φ_{ES} and φ_S were comparable. For the sample length of 4 mm in the temperature range of impurity scattering and excitation intensity ~ 10 W/cm^2, the measured potentials have the level of 10^{-5} V. The amplitude of φ_{ES} was found to be independent of the mechanical boundary conditions, while φ_S exceeds φ_{ES} by 8 dB for a "matched" boundary and by 14 dB for an almost free boundary. The dependencies of the amplitude and phase of φ_{ES} and u_{ES} on the temperature (i.e., on the electron scattering rate), measured in the same sample in the normal state, are shown in Fig. 1. We draw one's attention to the qualitative difference between the behavior of the phases for these components, which seems to be a decisive test for possible theories, as we will see below. The temperature changes of the amplitude and phase of φ_S are shown in Fig. 2. In contrast to analogous data presented in Ref. 1, the potential $\varphi_S(T)$ shows a more complicated nonmonotonic behavior, which indicates interference of nearly antiphase signals, φ_q and φ_{qw}, whose amplitudes have different dependencies on the electron scattering intensity.[1]
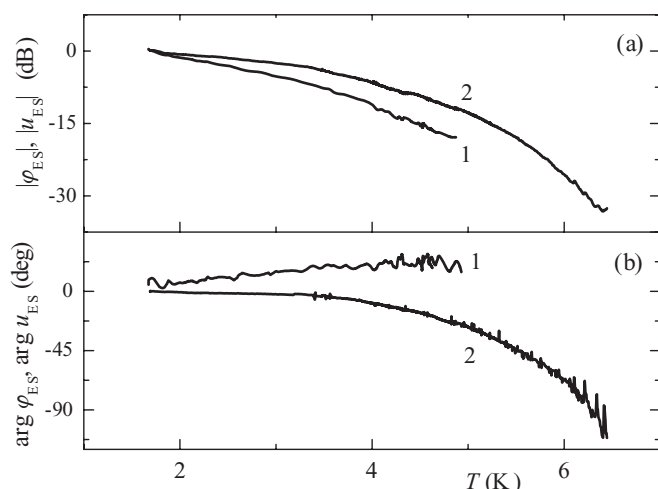

FIG. 1. Amplitudes (a) and phases (b) of the potential φ_{ES} (curves 1) and elastic displacement u_{ES} (curves 2) in the electron sound wave vs temperature.
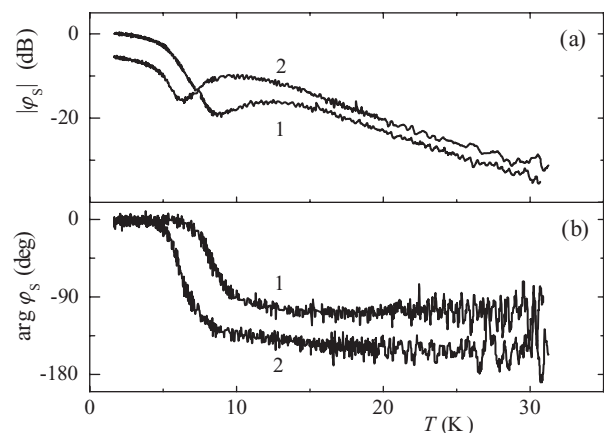

FIG. 2. Amplitude (a) and phase (b) of the potential φ_S of the acoustic wave vs temperature; curves 1 are for the "almost free" interface and curves 2 are for the "almost matched" interface.

III. THEORETICAL ANALYSIS

A. Free-electron model

As in Ref. 1, we first analyze a free-electron model by using a slightly different approach, which is consistent with the scheme of the experiment and enables simultaneous calculations of the potentials φ_{ES} and φ_S. We consider a metal plate with the thickness x_0, subjected by elastic vibrations with the amplitude u_0 at the face $x = 0$, and calculate φ_{ES} and φ_S at $x = x_0$. For simplicity, we assume the same densities ρ and sound velocities s for the delay line, the receiving electrode and the sample. The system of equations[19] consists of the one-dimensional linearized kinetic equation in the relaxation time approximation [the time dependence is chosen as $\exp(i\omega t)$],

$$i\omega\psi + v\frac{d\psi}{dx} + \nu\psi = -i\omega\Lambda\frac{du}{dx} + ev\frac{d\varphi}{dx}, \quad (1)$$

the equation of the elasticity theory,

$$-\rho\omega^2 u = \rho s^2 \frac{d^2 u}{dx^2} - \frac{dW}{dx}, \quad W = \langle \Lambda\psi \rangle, \quad (2)$$

and the electroneutrality condition

$$\langle \psi \rangle = 0. \quad (3)$$

Here, ψ is a nonequilibrium addition to the distribution function, u is the elastic displacement, v is the x component of the Fermi velocity, Λ is the longitudinal part of the deformation potential ($\Lambda = \lambda - \langle\lambda\rangle / \langle 1\rangle$, $\lambda = -mv^2$), ν is the relaxation frequency,

$$\varphi = \varphi_E + \frac{1}{e}\frac{du}{dx}\frac{\langle\lambda\rangle}{\langle 1\rangle} - \frac{m\omega^2}{e}\int_0^x u\,dx \quad (4)$$

is a full electrochemical potential measured by a voltmeter, φ_E is its electrical component satisfying Maxwell's equations. The last term in Eq. (4) describes a small Stewart-Tolmen's effect, which can be ignored for all cases analyzed below. The angle brackets denote averaging over the Fermi surface,

$$\langle A \rangle \equiv \frac{2}{h^3}\int \frac{A\,dS}{v_F}.$$

Equations (1) and (3) lead to the condition of the absence of the longitudinal current,

$$\langle v\psi \rangle = 0. \tag{5}$$

The condition of completely diffusive reflection of electrons for the boundary $x = 0$ has the form

$$\psi(x = 0) = \begin{cases} \psi_0(v), & v < 0, \\ C_0 = \text{const}, & v > 0, \end{cases} \tag{6}$$

and similarly for $x = x_0$. The function ψ_0 and the constant C_0 must be found self-consistently.

Typically, such a problem is solved by the representation of the solution of Eq. (1) through an integral formula,[16,20] with subsequent solution of integrodifferential equations by the Wiener-Hopf method.[21] We will use a more simple implementation of this method: extending the solution to the whole x axis and assuming all fields outside the interval $(0, x_0)$ to be zero, we apply the integral Fourier transformation

$$A_k = \int_0^{x_0} A(x) \exp(-ikx) dx, \quad A(x) = \int_{-\infty}^{\infty} A_k \exp(ikx)\frac{dk}{2\pi}$$

directly to Eqs. (1)–(3). The Fourier transform of the kinetic equation (1) reads as

$$\psi_k(L + ik) - \omega k \frac{\Lambda}{v} u_k - iek\varphi_k$$

$$- \left[-i\omega \frac{\Lambda}{v} u(x_0) + e\varphi(x_0) - \psi(x_0)\right] e^{-ikx_0}$$

$$= -i\omega\frac{\Lambda}{v}u(0) - e\varphi(0) + \psi(0), \quad L = \frac{i\omega + v}{v} \equiv \frac{i\widetilde{\omega}}{v}. \tag{7}$$

To ensure the validity of Eq. (7) in the entire complex plane of k, the functions ψ_k, u_k, and φ_k should have components proportional to the factor $\exp(-ikx_0)$, which compensate the last term in the left-hand side of Eq. (7). A similar conclusion relates to the Fourier transforms of Eqs. (2) and (3). Thus the system splits into two blocks, with and without the exponential factor; however, direct application of the Wiener-Hopf procedure to these blocks is impossible, which can be demonstrated by a simple example. The above defined Fourier transform of any wave mode propagating with attenuation in the forward $(+)$ or backward $(-)$ direction in the interval $(0, x_0)$, having initial amplitudes $A_0^+ = A^+(0)$ or $A_0^- = A^-(x_0)$, respectively, is given by

$$A_k^{\pm} = \frac{A_0^{\pm}}{i(\pm r - k)}[e^{i(\pm r - k)x_0} - 1]. \tag{8}$$

Here, r is the complex wave number located, e.g., for the direct $(+)$ wave in the second quadrant. The Fourier components of the fields, representing a separate solution for each block, generally contain both direct and backward waves, therefore they have singular points in the upper and lower half-planes, as follows from Eq. (8). The Wiener-Hopf method is not applicable to such functions.

In order to get around this difficulty, we group the terms in each block obtained from Eq. (7) according to the location of their singular points, i.e., divide the full solution for each block into the forward and backward waves. The values of the fields

at the interfaces $x = 0$ and x_0 also contain partial contributions of the direct and backward waves, $A(0) = A^+(0) + A^-(0)$ (and similar for $x = x_0$), which are to be attached to the related groups. Taking into account the existence of the common band of analyticity $-\text{Im}\,r < \text{Im}\,k < \text{Im}\,r$ for these two groups and the relation $kA_k|_{k\to\infty} = iA(0)$ for each partial component, and using the Liouville's theorem,[21] we conclude that each of these groups is equal to 0. After such a separation, the Wiener-Hopf method is already applicable, and we come to the conclusion that in the case of diffusive sample boundaries, the response to an external perturbation at the receiving interface is a combination of solutions for the forward and backward waves in the half-space with corresponding partial amplitudes of the perturbing signals. The relation between these amplitudes is to be found from the continuity conditions for the displacements and stresses at the boundary.

By using these considerations, we address the equations for the forward wave, obtained from the Fourier transforms of Eqs. (1)–(3) after the separation procedure. After some algebra, we get the relation between u_k and φ_k in the forward wave (we omit the upper index $+$),

$$(k^2 - q^2)u_k + i\zeta ek\varphi_k\lambda_0^{-1} = -iku_0 + C_1. \tag{9}$$

Here and below, the symbol C_i ($i = 1,2$) denotes combinations of the fields at the exciting interface (the single used property of C_i is their independence of k), $\lambda_0 = mv_F^2$, $\zeta = \lambda_0/Ms^2 \sim 1$, M is the ion mass. Eliminating φ_k from Eqs. (3) and (9), we arrive at the equation for u_k,

$$Z(k)[kBu_k - u_0(B + q^2) + kC_2] = A(-q^2u_0 + kC_2)$$

$$- \frac{B\zeta}{\lambda_0}\left(\left\langle\frac{\psi_0}{L + ik}\right\rangle_{v<0} - \left\langle\frac{C_0}{L + ik}\right\rangle_{v<0}\right),$$

$$Z(k) = A + BJ, \quad A = \frac{k_\omega\zeta}{3k_0}, \quad k_\omega = \frac{\omega}{v_F}, \quad k_0 = \frac{\widetilde{\omega}}{v_F},$$

$$B = k^2 - q^2 + k_\omega\zeta\left(k_0 + \frac{k^2}{3k_0}\right), \quad q = \frac{\omega}{s}, \tag{10}$$

$$J = \frac{1}{\langle 1\rangle}\left\langle\frac{1}{L^2 + k^2}\right\rangle = \frac{1}{k^2} - \frac{k_0}{2k^3}\ln\frac{k_0 + k}{k_0 - k}.$$

In derivation of Eq. (10), we used the following chain of transformations,

$$\left\langle\frac{\psi(0)}{L + ik}\right\rangle = \left\langle\frac{\psi_0}{L + ik}\right\rangle_{v<0} + \left\langle\frac{C_0}{L + ik}\right\rangle_{v>0}$$

$$= \left\langle\frac{\psi_0}{L + ik}\right\rangle_{v<0} - \left\langle\frac{C_0}{L + ik}\right\rangle_{v<0} + C_0J. \tag{11}$$

We emphasize that the possibility to take the factor C_0 out of the averaging in Eq. (11) determines the applicability of the Wiener-Hopf method to our problem. We also note that the combination in the curly brackets in Eq. (10) plays the role of a "fictitious" function appearing in this method.

The characteristic function $Z(k)$ determines the spectrum of the wave numbers of the propagating modes. In our simplest case, the equation $Z(k) = 0$ has only a pair of the roots $r_{\pm} = \mp q \pm i\alpha_L$, corresponding to the acoustic wave renormalized by interaction with electrons. At $q\ell \gg 1$, the attenuation decrement $\alpha_L = \pi k_\omega/12$ represents the Landau damping independent of the mean free path $\ell = v_F/v$. Besides,

the function $Z(k)$ has a pair of the branch points $k = \pm k_0$ associated with the quasiwave (ballistic) process with the propagation velocity close to v_F. The function $Z(k)$ has no singular points near the real axis within the band $-\delta < \text{Im} k < \delta$, $\delta = \min(\alpha_L, \ell^{-1})$, and turns to unity at $k \to \infty$. These properties enable us to factorize $Z(k)$ by using a standard procedure,[21] i.e., to present it as a product of the functions $T^+(k)$ and $T^-(k)$, analytical at $\text{Im} k > -\delta$ and $\text{Im} k < \delta$, respectively. In particular,

$$T^+(k) = \exp\left[\frac{1}{2\pi i}\int_{-\infty-i\gamma}^{\infty-i\gamma}\frac{\ln Z(\xi)}{\xi - k}d\xi\right], \quad \gamma < \delta. \quad (12)$$

This function can be calculated by the methods of contour integration. In the lower half-plane, the integrand in Eq. (12) has two branch points: $\xi = k_0$ from the internal logarithm in $Z(\xi)$ and $\xi = r_-$, in which the function $Z(\xi)$ turns to zero. We make a cut for the internal logarithm along the ray $\xi = k_0 y$ $(1 < y < \infty)$. Since the function $Z(\xi)$ is regular at $\xi = 0, \infty$, the second cut, beginning at the point $\xi = r_-$, is finished at some point $\xi = r_0$ belonging to the first cut. Then, tracing the cuts and calculating corresponding contour integrals, we get

$$T^+(k) = \frac{k - r_-}{k - r_0}\tau^+(k), \quad (13)$$

where $\tau^+(k)$ is the contribution of the cut of the internal logarithm,

$$\tau^+(k) = \exp\left[\frac{k_0}{2\pi i}\int_1^\infty\frac{\ln Z(k_0 y + 0i) - \ln Z(k_0 y - 0i)}{k - k_0 y}dy\right]. \quad (14)$$

The value of r_0 can be found assuming $k = 0$ in Eq. (12). In this limit, after displacement of the integration contour to the real axis, the principal value of the integral vanishes and only the contribution $\pi i \ln Z(0)$ of the trace around the coordinates origin survives. Comparing this result with Eq. (13), we get $r_0 = r_-\tau^+(0)Z^{-1/2}(0)$. Note that the formal singularity in Eq. (13) at $k = r_0$ is removable, because $\tau^+(k)_{k \to r_0} \to 0$.

Dividing Eq. (10) over $T^+(k)$, we obtain a functional equation with the right-hand and left-hand sides analytical at $\text{Im} k > -\gamma$ and $\text{Im} k < \gamma$, respectively. Due to the Liouville's theorem, they can be presented as a first power polynomial $A(\alpha k + \beta)$, and we obtain the final expression for the Fourier image of the elastic displacement in the forward wave:

$$u_k = \frac{A(\alpha k + \beta)T^+(k)}{ik B(k)Z(k)}. \quad (15)$$

According to Eq. (5), the combination in curly brackets in Eq. (10) vanishes at $k = 0$, which gives $\beta = \sqrt{3}qk_0u_0$. Expression for the parameter α follows from Eq. (10) at $k = \pm b$, where b is a root of the equation $B(k) = 0$. Note that we omitted the terms in Eq. (15), which are inessential for the calculation of $u(x)$ [they eliminate nonphysical poles in Eq. (15) at $k = 0, \pm b$ and give zero contribution to the inverse Fourier transform of u_k].

According to Eq. (15) and the properties of the function $Z(k)$ described above, the forward wave consists of two modes having different velocities: the quasiwave and the sound wave. Elastic displacements in these excitations, $u_{qw} \sim (s/v_F)^2 u_0$ and $u_q \sim u_0$, respectively, differ by 4–5 orders of magnitude.

However, the electric potentials excited by these modes are comparable by their magnitudes,

$$\varphi_q \sim \varphi_{qw} \sim \frac{k_\omega \lambda_0}{e}u_0. \quad (16)$$

These estimations follow from Eq. (9) at $k = q + i\alpha_L$, $u \sim u_0$ for the sound wave and $k \approx k_\omega$, $u \sim (s/v_F)^2 u_0$ for the quasiwave. Comparing Eq. (16) with Eq. (4), we conclude that the resulting sound potential is formed by practically complete ($\sim s/v_F$) cancellation of two large terms. On the contrary, the quasiwave potential is mainly represented by the electric component.

Now we consider the values of the fields registered at the receiving interface. The excitation incoming at the sample boundary $x = x_0$ produces its deformation, which is the source of backward waves. Their behavior is described by similar equations with substituting u_0 by the partial amplitude $\tilde{u}(x_0)$, whose value can be found from the mechanical boundary conditions. The measured potential is the sum of contributions of the forward and the backward waves. As an example, we find the elastic displacement and the potential created by a direct quasiwave, coming with the amplitude $u_{qw}(x_0)$ to the matched interface. In this case, evaluation of the integral in Eq. (14) is required; however, we will use instead the characteristic values of $k \sim k_0 \ll q$ for estimations. For the backward waves, the quasiwave contribution is negligible, and we should take into account only the acoustic component. In this approximation, the conditions of equality of displacements and stresses for both sides of the interface read as

$$u_{ES} = u_{qw} + \tilde{u}(x_0), \quad \tilde{u}(x_0) \approx \frac{1}{2iq}\frac{W_{qw}(x_0)}{\rho s^2} - \frac{u_{qw}}{2}, \quad (17)$$

$$-iqu_{ES} = ik_0u_{qw}(x_0) + iq\tilde{u}(x_0) - \frac{W_{qw}}{\rho s^2}. \quad (18)$$

Here, u_{ES} is the amplitude of displacements created by the electron sound signal in a load (including the receiving piezotransducer). The electronic pressure for a direct quasiwave can be found from the Fourier transform of Eq. (2),

$$\frac{W_{qw}}{\rho s^2} \approx \frac{q^2 - k^2}{ik}u_{qw}(x_0). \quad (19)$$

As a result, we obtain $u_{ES} \approx \tilde{u}(x_0) \approx (q/2k_0)u_{qw}(x_0) \sim (s/v_F)u_0$, i.e., the displacement amplitude at the receiving interface exceeds its value in the incoming wave of the electron sound by a large factor v_F/s.[14] At the same time, the potential created by the backward waves is small, thus, φ_{ES} equals to the potential of a direct quasiwave $\varphi_{qw}(x_0)$. Although the quantity $\tilde{u}(x_0)$ at the free boundary is twice as large, the contribution of backward waves can be also neglected in this case. This means that the amplitude of φ_{ES} is practically independent of the mechanical boundary conditions, in agreement with our experiments.

For the sound potential, the cases of the matched and the free boundaries differ in essence. In the first case, the quantity $\tilde{u}(x_0)$ is small by the parameter α_L/q, thus the contribution of the secondary waves is negligible, and $\varphi_S(x_0)$ equals to the potential of the primary sound wave. For the free interface, $\tilde{u}(x_0)$ coincides with the amplitude of the incident wave, their potentials are fully compensated, and only the potential of the secondary quasiwave survives. In the regime of the impurity

scattering (low-temperature limit), the quasiwave contribution exceeds the acoustic one by the factor of 1.5 (for the specular boundary,[1] φ_{qw} exceeds φ_q by a factor more than 3). When the electron scattering increases, the acoustic component φ_q always becomes prevalent.

The experimental dependencies in Fig. 2 qualitatively agree with the estimations given above. Of course, the used variants of measurement of the potential cannot be attributed to the purely matched or free boundary, therefore both the acoustic and quasiwave contributions are present in φ_S. Nevertheless, we note that in the regime of the impurity scattering, φ_S is larger for the variant more close to a free boundary case than for a matched one. And vice versa, in a high-temperature region, only φ_q remains, and a more intensive signal is observed in the "matched" variant.

Within the same model, we analyze the case of a specular receiving interface, assuming the exciting interface to be diffusive to avoid possible resonant effects. Different authors used various approaches to similar problems (see, e.g., Ref. 20) but they actually exploit an identical procedure—replacement of the interface by a specularly inverted sample. The scalars in the fictitious sample are the same as in the real one, the x components of polar vectors change their signs, and the tensor functions are transformed in accordance with the usual rules. Due to the specular reflection conditions, the distribution function is continuous at $x = x_0$.

Applying the Fourier transformation [now within the interval $(0, 2x_0)$, out of which all fields are assumed to be equal to 0] to our system, we conclude that the complete solution splits into three blocks [cf. with Eq. (7)]. One of them (without the exponential factor) coincides with the one discussed above and describes the waves generated at the interface $x = 0$. Two others [$\sim \exp(-2ikx_0)$ and $\sim \exp(-ikx_0)$] are virtual excitations, but their sum determines real backward waves. The first of these terms is the "specularly inverted" wave, in accordance with the rules accepted. Obviously, at $x = x_0$, this wave produces a displacement opposite in phase and a potential of the same sign compared to those in the incoming wave. The second term is the excitation generated by complete (not partial!) displacements $u(x_0)$ of the interface. In our notations, its Fourier transform is

$$u_k = -\frac{2Aq^2 u(x_0)}{ik\, B(k)Z(k)}, \qquad (20)$$

where we omitted inessential terms, which cancel out the poles at $k = 0, \pm b$, similar to Eq. (15). The potential is determined by Eq. (9) with minor modification of the right-hand side. If one considers $u(x_0)$ as an independent value, then Eqs. (15) and (20) determine the relationship between the amplitudes of displacements generated at the diffusive and specular boundaries, respectively. For the acoustic mode, it is very close to 1, while for the quasiwave this relation is about 0.5.

In analysis of the mechanical boundary conditions, all three solutions must be taken into account. Obviously, the sum of first two solutions gives zero displacement and doubled potential and electronic pressure. In the case of a quasiwave incident on the specular interface, the corrections arising from the backward waves are small, therefore the full potential φ_{ES} at the specular interface is twice as large than at the diffusive one.

In the case of the sound wave incident on the matched interface, the quantity $u(x_0)$ coincides with the incoming signal. Summing up the solutions, we find the potential created by the acoustic wave and an additional potential generated by the quasiwave. The relationship between these contributions coincides with that calculated before.[1] The amplitude of displacements in the backward sound wave is small because of practically full cancellation of the second and third terms.

Thus, for the specular interface, the potentials φ_{ES} and φ_S exceed, as a rule, their values for the diffusive case. The only exception is a hypothetical fully fastened surface, $u(x_0) = 0$; in the diffusive case, both the doubled potential φ_q and φ_{qw} contribute to φ_S, while for the specular interface, the term φ_{qw} is absent. It is also worth noticing that there is a qualitative difference between the diffusive and specular cases for the matched interface in the clean limit $q\ell \gg 1$; the contribution to φ_S from the quasiwave for a diffusive boundary is practically absent, while it dominates in a specular case.

B. Multiband models

Despite the successful explanation of several important experimental facts, the free-electron model has an essential drawback: it does not explain the difference between the phases of φ_{ES} and u_{ES} clearly seen in Fig. 1(b). Indeed, comparing Eqs. (9) and Eqs. (17), (19), we see that the electron sound potential and elastic displacements at the interface are described by expressions, similar up to a scale factor. It seems that the consideration of the quasiwave as a single carrier of the electron sound will lead to an analogous conclusion for any modification of the approach.

However, the quasiwave is not a unique mechanism of the electron sound transport. In the presence of strong enough Fermi-liquid interaction (FLI) and several sheets of the Fermi surface with close Fermi velocities but different values of the deformation potential, the excitation of zero sound in metal is possible.[8–13] It was found[14,15] that a considerable change in the phase of the elastic component of the electron sound in Ga with temperature is related to the change of its velocity, associated with the crossover from the collisionless propagation of the zero sound to the concentration wave regime[15,17] (the electron analog of ordinary sound). Theoretical analysis, based on the model of a compensated metal with two equivalent zones showed that the necessary condition for such a crossover is relatively weak interband scattering.[15] This requirement is not an artificial limitation of the model, since the interband gaps are often large enough, therefore in the actual range of temperatures, the interband transitions are only due to rare electron-impurity or electron-electron collisions. At the same time, the intraband relaxation above the crossover temperature is determined by much more frequent electron-phonon collisions.

Within this model, the elastic component of the zero sound (or concentration mode) predominates the ballistic one at reasonable values of the FLI parameters, but the potentials φ_{ES} and φ_S are identically zero. For their emergence, a certain asymmetry must be introduced: unequal FLI coefficients, different densities of states, or different (but close) values of the Fermi velocities. However, in this case, the phase of the zero sound potential behaves similar to the phase of the elastic

component. Thus, the two-band model also cannot give any explanation of the data presented in Fig. 1(b).

A qualitative interpretation of these data can be obtained within the framework of a three-band model. We represent the Fermi surface by three spheres of identical sizes, two of which are of the electron type and one of the hole type (or vice versa). The Fermi velocities, the densities of states, the relaxation rates, and the intensity of FLI are supposed to be equal for all bands. Besides, we assume the absence of interband transitions caused by the electron-phonon scattering and equality of the rates of the intra- and interband impurity scattering. Under these assumptions, the kinetic equation in each band ($i = 1,2,3$) for the distribution function renormalized by FLI[14,15] has a form similar to Eq. (1), with an additional force term in the right-hand side,

$$i\widetilde{\omega}\psi_i + v\frac{d\psi_i}{dx} + \nu\psi = -i\omega\Lambda_i\frac{du}{dx} + ev_i\frac{d\varphi}{dx} + \frac{\omega^-}{\langle 1 \rangle}\langle\psi_i\rangle,$$
(21)

where F is the difference of the isotropic parts of Landau correlation functions for the intra- and interband FLI, $\omega^- = \nu_{ph} + i\omega F/(1 + F)$, $\nu = \nu_{ph} + 3\nu_{imp}$, ν_{ph} and ν_{imp} are the frequencies of the intraband electron-phonon and electron-impurity collisions, respectively. The FLI renormalizes the function W in Eq. (2) as well,

$$W = \sum_i \left(\langle\Lambda_i\psi_i\rangle - \frac{F}{1 + F}\langle\Lambda_i\rangle\frac{\langle\psi_i\rangle}{\langle 1 \rangle} \right),$$

and Eqs. (3) and (5) take the form $\sum_i\langle\psi_i\rangle = 0$ and $\sum_i\langle v_i\psi_i\rangle = 0$.

As well as in the two-band model,[8,9,11] these equations have a zero-sound solution transformed into the concentration mode with the increase of scattering. The results, obtained for the specular receiving interface, show that for reasonable intensity of FLI ($F \sim 1$), the elastic and potential components of the electron sound in this case are formed by different
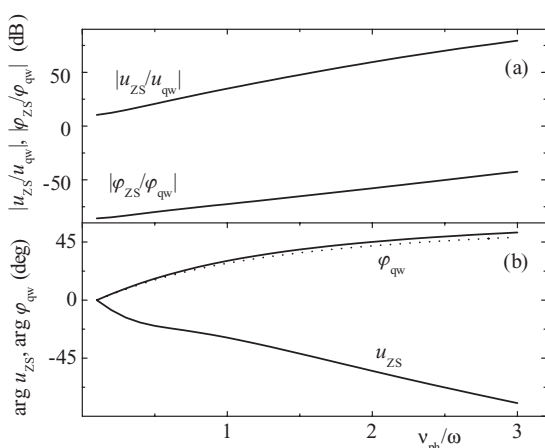

FIG. 3. Calculated relations (a) of the amplitudes of elastic displacements and potentials for separate components of electron sound vs electron-phonon scattering rate in the three-band model and (b) of computed phases of the dominant components. The following parameters are used: $\zeta = 1$, $F = 1$, and $\omega/3\nu_{imp} = 5$. Dotted line is the phase of the quasiwave components for the free-electron model.

mechanisms. Indeed, as is obvious from Fig. 3(a), the elastic component u_{ZS} of the zero sound much exceeds its value in the quasiwave and, at the same time, the quasiwave potential dominates. As a result, the behavior of the phases of dominant components presented in Fig. 3(b) qualitatively agrees with the experimental data shown in Fig. 1(b).

The behavior of the phase of the quasiwave potential, following from the one-band model with the diffusive surface, is also presented in Fig. 3(b). Almost complete coincidence of these results with the ones for the three-band model indicates insensitivity of the phase of quasiwave solutions to the particular choice of the model and to the character of electron scattering at the interface.

IV. BEHAVIOR OF POTENTIAL IN SUPERCONDUCTING PHASE

The algorithm of calculation of the potential in the superconducting phase is similar to the procedure described in Sec. III. In particular, the same equations of elasticity, electro- and current neutrality are used. Of course, the calculation of corresponding averages is much more difficult due to the energy dependence of both the velocity of normal excitations and the relaxation frequencies.[1,22] However, in derivation of Eq. (9) within the free-electron model, no specific calculations of the kinetic coefficients were performed, therefore the structure of Eq. (9) holds in the superconducting state as well. This means that φ_q cannot decrease below T_c faster than the sound attenuation decrement $\alpha_L(T)$ (for the case of a specular interface, a detailed analysis was given in Ref. 1). Moreover, since the sound attenuation in our sample is rather large, $\alpha_L x_0 > 1$, the dependence $\varphi_q(T)$ must pass through a maximum due to rapid increase of the damping factor $\exp[-\alpha_L(T)x_0]$ near T_c. The relationship similar to Eq. (9), following from the elasticity equation, occurs in any model, therefore the conclusion about the temperature dependence of φ_q seems to be always true.

However, as it has been already reported,[1] the experimental value of φ_S decreases considerably faster than expected on the basis of these considerations. We note that the measurement of the potential in these experiments was carried out by a point contact, for which the mechanical boundary conditions depend on its pressing, i.e., on a badly controlled parameter. In particular, it can be thought that the situation with a point contact is close to the case of free boundary, and, correspondingly, the contribution of φ_q in the potential measured in Ref. 1 is completely absent. In the present experiments, φ_q is unambiguously a part of φ_S; nevertheless, the result of measurements of $\varphi_S(T)$ in the superconducting state shown in Fig. 4 completely reproduces the previous result.

At large excitation intensity, $|\varphi_S(T)|$ exhibits a maximum, which is due to local overheating of the receiving interface and vanishes with the decrease of u_0. In the absence of the overheating, the quantity $|\varphi_S(T)|^{-1}$ obeys the law close to linear in $\Delta T = T_c - T$ (see Fig. 4, inset) with a large prefactor similar to that in the imaginary part of the transversal conductivity of a superconductor, $\mathrm{Im}\sigma_s/\sigma_n \approx (2v_F/s)(\Delta T/T_c)$, which describes screening of the electromagnetic field of the sound wave by supercurrents. This enables one to suspect that the oscillating currents, spreading over the sample surface
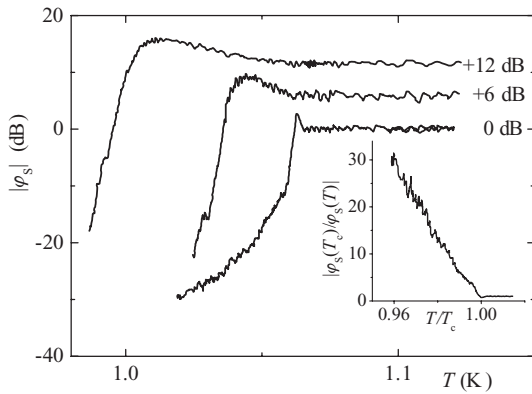
FIG. 4. Amplitude of the sound wave potential φ_S vs temperature below T_c at different levels of the exciting signal. Inset: behavior of $|\varphi_S(T)|^{-1}$ in a near vicinity of T_c for the curve 0 dB.

from the sound spot, take part in formation of $\varphi_S(T)$. These currents were indeed observed in the experiments;[1] however, they disappear at $T < T_c$ as quickly as the potential does and therefore hardly can be a primary cause of its decrease.

Generally, the theoretical analysis of $\varphi_S(T)$ and the interpretation of its experimental behavior represent a rather complicated problem, because both φ_q and φ_{qw} contribute to the sound potential. In principle, these terms may compensate each other, although such a situation seems to be hardly probable. Moreover, as was noted above, the potential φ_q is the result of practically complete ($\sim s/v_F$) cancellation of large electric and deformation contributions; for this reason, the ordinary accuracy of estimations (also $\sim s/v_F$) must be substantially increased. In this sense, the measurement of φ_{ES} is more preferable, because this potential has a purely electric nature. The results of measurements of $\varphi_{ES}(T)$ and $u_{ES}(T)$ presented in Fig. 5 show that the potential of the electron sound disappears at $T < T_c$ practically in a jumplike way, similar to φ_S. Strangely, but the result of measuring φ_S and φ_{ES} looks as an evidence of impossibility of the existence of the potential gradient in a superconductor. Of course, we do not adhere to such a point of view, because it fully contradicts the universally recognized theories and well established experimental facts
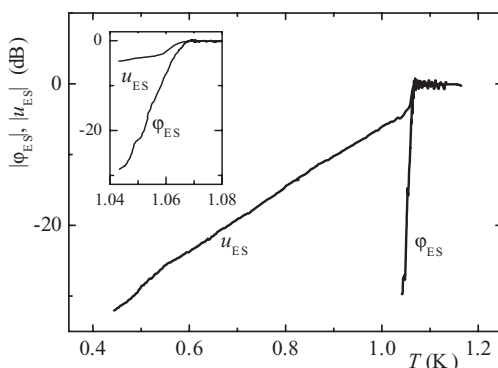

FIG. 5. Changes of the amplitudes of the potential and elastic displacement in the electron sound wave below T_c. Inset: expanded scale near T_c.

(see, e.g., a review[18]), but the problem of interpretation of these paradoxical data still exists.

The nature of the signal $u_{ES}(T)$ also remains unclear. Taking into account the analysis of the three-band model, it could be thought that a small jump in $u_{ES}(T)$ near T_c (see Fig. 5) can be interpreted as the suppression of the quasiwave just below T_c. Furthermore, it was shown experimentally[14] that the change of both the amplitude and the phase of $u_{ES}(T)$ below T_c has nothing to do with the change of attenuation and velocity of the electron sound and relates only to the behavior of the coefficient of coupling between the electron sound and the exciting elastic deformation. This contradicts the theoretical predictions[22] about the behavior of the quasiwave amplitude and phase in the superconductor. Besides, we would remind the conclusion of Ref. 23 that in presence of the interband Cooper pairing, the zero sound spectrum in the superconducting phase has an activating character with a gap close to the energy gap of the superconductor. Thus the propagation of the zero sound at our frequencies is forbidden in the superconducting state. But if the signal $u_{ES}(T)$ below T_c is neither zero sound nor the quasiwave, then what is it? No clear answer on this question exists yet.

V. CONCLUSION

We have measured the temperature dependencies of the amplitude and the phase of the potential φ_{ES} and the elastic displacement u_{ES} accompanying a fast electron sound wave excited by the longitudinal ultrasound in a single crystal of high-purity Ga. Simultaneously, the amplitude and the phase of the potential φ_S and the elastic displacement u_S in the excited acoustic wave have been studied. We found that in the normal state, the behavior of the phases of φ_{ES} and u_{ES} differs qualitatively: while the phase of φ_{ES} increases with temperature, the phase of u_{ES} decreases. By using the Wiener-Hopf method, we examined several theoretical models that describe excitation and propagation of different types of the electron sound in samples of finite size with the diffusive exciting interface.

The model of free electrons, in which only the quasiwave is responsible for the electron sound transport, enabled us to explain several important experimental facts: giant enhancement (by the factor v_F/s) of elastic displacements induced by the electron sound wave at the sample boundary, insensitivity of φ_{ES} on the boundary conditions at the receiving interface, and the temperature behavior of φ_S and its closeness to φ_{ES} in the magnitude. However, neither this model nor the model of a compensated metal with two sheets of the Fermi surface (in which zero-sound or concentration modes occur in presence of the Fermi-liquid interaction) are able to explain the difference between the phases of φ_{ES} and u_{ES}.

We obtained a qualitative interpretation of this experimental result within a model with three equal Fermi spheres, which reflects the presence of three main sheets of the Fermi surface in Ga.[24] For reasonable values of the Fermi-liquid interaction coefficients, the elastic signal u_{ES} was found to be formed by the zero sound, while the potential φ_{ES} is basically associated with the quasiwave, which results in opposite changes of their phases with temperature. Of course, this simple model cannot pretend to be a quantitative description of the real

situation. Nevertheless, our estimations indicate a possibility, in principle, for the "potentialless" propagation of the zero sound (or the concentration wave) on a background of the potential created by the ballistic transport and enable us to suppose actual realization of a similar scenario in the experiments.

Below the temperature of the superconducting transition, we observed a sharp disappearance of the potential of both the electron sound wave and the acoustic wave, which contradicts our theoretical estimations and generally adopted conceptions of the behavior of the longitudinal electric field in superconductors. The origin of this puzzling effect, as well as the nature of the elastic signal of the electron sound in the superconductor, is not clear yet.

[1] Yu. A. Avramenko, E. V. Bezuglyi, N. G. Burma, I. G. Kolobov, V. D. Fil, O. A. Shevchenko, and V. M. Gokhfeld, Low Temp. Phys. **28**, 328 (2002); Mater. Sci. Eng. A **370**, 373 (2004).

[2] R. H. Parmenter, Phys. Rev. **89**, 990 (1953).

[3] G. Weinreich and H. G. White, Phys. Rev. **106**, 1104 (1957).

[4] N. V. Zavaritskii, Sov. Phys. JETP **48**, 942 (1978).

[5] D. Pines, Can. J. Phys. **34**, 1379 (1956).

[6] G. I. Ivanovski and M. I. Kaganov, Sov. Phys. JETP **56**, 1345 (1982).

[7] L. P. Gor'kov and I. E. Dzyaloshinskiĭ, Sov. Phys. JETP **17**, 111 (1963).

[8] S. Z. Dunin and E. P. Fetisov, Sov. Phys. Solid State **14**, 221 (1972).

[9] V. M. Dubovik and E. P. Fetisov, Solid State Commun. **13**, 1669 (1973).

[10] N. G. Burma, E. Yu. Deineka, and V. D. Fil, JETP Lett. **50**, 20 (1989).

[11] E. V. Bezuglyi, N. G. Burma, E. Yu. Deineka, and V. D. Fil, Physica B **173**, 405 (1991).

[12] E. V. Bezuglyi, N. G. Burma, V. D. Fil, E. Yu. Deineka, and H.-J. Kaufmann, J. Phys. Condens. Matter **3**, 7867 (1991).

[13] E. V. Bezuglyi, N. G. Burma, V. D. Fil, E. Yu. Deineka, and A. I. Kopeliovich, J. Low Temp. Phys. **91**, 179 (1993).

[14] Yu. A. Avramenko, E. V. Bezuglyi, N. G. Burma, and V. D. Fil, Low Temp. Phys. **35**, 724 (2009).

[15] E. V. Bezuglyi, N. G. Burma, E. Yu. Deineka, and V. D. Fil, Low Temp. Phys. **19**, 667 (1993).

[16] V. M. Gokhfeld, Low Temp. Phys. **29**, 41 (2003).

[17] A. I. Kopeliovich and M. S. Churiukin, Low Temp. Phys. **19**, 125 (1993).

[18] S. N. Artemenko and A. F. Volkov, Physics-Uspekhi **22**, 295 (1979).

[19] V. M. Kontorovich, Sov. Phys.-JETP **18**, 1125 (1964).

[20] A. A. Abrikosov, *Fundamentals of the Theory of Metals* (North-Holland, Amsterdam, 1988).

[21] B. Noble, *Methods Based on the Wiener Hopf Technique* (Pergamon Press, New York, 1959).

[22] E. V. Bezuglyi and A. V. Boichuk, Low Temp. Phys. **23**, 507 (1997).

[23] A. J. Leggett, Prog. Theor. Phys. **36**, 901 (1966).

[24] W. A. Reed, Phys. Rev. **188**, 1184 (1969).